*Short Communication*

# Effects of Nanosized Nb Carbide Precipitates on the Corrosion Behavior of High-Strength Low-Alloy Steel in Simulated Seawater

*Qiyue Zhao[1], Zihao Wang[1], Endian Fan[1], Xiaoguang Wu[1], Yunhua Huang[1,\*] , Xiaogang Li[1,2]*

[1] Corrosion and Protection Center, University of Science and Technology Beijing, Beijing 100083, China
[2] Ningbo Institute of Material Technology & Engineering, Chinese Academy of Sciences, Ningbo 315201, Zhejiang, China
[\*]E-mail: huangyh@mater.ustb.edu.cn

Nb is usually utilized in high-strength low-alloy (HSLA) steels as a strengthening and toughening microalloying element. HSLA steels with different Nb contents, or different amounts of precipitates were chosen to study the effects of Nb and Nb carbide precipitates on the corrosion behavior of HSLA steel in simulated seawater respectively. Microstructural and electrochemical investigations revealed that Nb enhances the corrosion resistance of HSLA steel due to the homogeneous microstructure resulted from NbC precipitation in steel. Moreover, although as a cathodic phase, the nano-sized Nb carbide precipitates have no deteriorating effect on the corrosion behavior of HSLA steel in simulated seawater.

**Keywords:** NbC precipitate; corrosion; HSLA steel; simulated seawater

## 1. INTRODUCTION

Nb has been widely exploited and utilized as a micro-alloying element in high-strength low-alloy (HSLA) steels, especially for high strength pipelines. Nb, Ti, and V micro-alloyed high strength steels have high strength and toughness, mainly due to grain refining and precipitation strengthening [1-3]. Niobium forms Nb(C,N) with high hardness and a high melting point, which is very effective in restraining the growth of austenite grains and inhibiting austenite recrystallization [4-6]. In addition, Nb(C,N) precipitates also improve the resistance of hydrogen-induced delayed fracture [7,8].

The main obstacle, seawater corrosion, must be confronted for HSLA steels used in offshore oil and ocean engineering. The effects of Nb microalloying on the microstructure and mechanical properties of steel have been widely studied [9,10]. Researchers agree that Nb can refine the grains of alloy steel, improve microstructure uniformity, and enhance mechanical and welding properties [11,12]. However, whether and how element Nb and the large number of nanoscaled niobium carbonitride precipitates affect the corrosion behavior of HSLA steel has not been fully understood, and requires further investigation.

In this work, with different Nb content, or a different amount of NbC precipitates, HSLA steel samples were investigated to reveal the effects of Nb and Nb carbide precipitates on the corrosion behavior of HSLA steel in simulated seawater, rather than the mechanical properties of the steels. The results will be beneficial for the development of Nb microalloying steel and the service safety of HSLA steel in ocean environments.

## 2. EXPERIMENTAL

Three types of HSLA steel with different Nb contents were used in this experiment. Table 1 shows the chemical compositions of the experimental steel.

**Table 1.** Chemical compositions of experimental steel (wt%)

|  | C | Si | Mn | P | S | Nb | Ti | Mo | Ni | Cu |
|---|---|---|---|---|---|---|---|---|---|---|
| Nb-free | 0.058 | 0.28 | 1.85 | 0.004 | 0.006 | 0 | 0.016 | 0.26 | 0.26 | 0.26 |
| Nb-bearing 1# | 0.061 | 0.28 | 1.87 | 0.004 | 0.006 | 0.079 | 0.016 | 0.26 | 0.26 | 0.26 |
| Nb-bearing 2# | 0.052 | 0.28 | 1.88 | 0.008 | 0.004 | 0.060 | 0.015 | 0.18 | 0.26 | 0.26 |

The experimental steels were produced by finishing rolling at 830°C and direct water-quenching. The sample of Nb-free steel was assigned as N1, and the sample of Nb- bearing 1# steel was assigned as N2. To obtain samples with the same content but different amounts of precipitates, the Nb-bearing 2# steel with 0.06wt% Nb content were added two different hot treatments, respectively, after rolling and quenching. First, the steel was heated to 1300°C, and held for 15 minutes to make the Nb carbide precipitates entirely dissolve in steel matrix. And then, the sample assigned as N3 was obtained by immediately quenching at 1300°C to the room temperature, and the sample assigned as N4 was quenched at 1000°C after the sample cooled with the furnace from 1300°C to the quenching temperature and held for 1 hour.

The microstructures of the samples were observed by optical microscopy (OM, Reichert-Jung Polyvar MET). In addition, and high resolution transmission electron microscopy Tecnai 30 (HRTEM) was used to observe the microstructures and nano-sized NbC precipitates.

Samples were ground using 2000 grit SiC sand paper, rinsed with distilled water and dried with ethanol, before electrochemical experiments. An electrochemical working station (VersaSTAT 3F, Princeton) was employed to conduct electrochemical measurements using a traditional three-electrode cell, with the sample as working electrode, a large area of the Pt plate as counter electrode, and a saturated calomel electrode (SCE) as the reference electrode. All electrochemical experiments were conducted in the simulated seawater solution, and Table 2 gives the main compositions. The electrochemical impedance spectroscopy (EIS) tests were applied with a potential amplitude of 10 mv for the open circuit potential measurements (OCP). A frequency range of 0.01-100000Hz was used for EIS experiments. The potentiodynamic polarization curves were measured in the potential region from -0.3 to 0.3V (vs. OCP) at a scanning rate of 0.5 mv/s.

**Table 2.** Chemical compositions of simulated seawater for electrochemical test solutions (g/L)

| NaCl | $MgCl_2$ | $Na_2SO_4$ | $CaCl_2$ | KCl | $NaHCO_3$ | $H_3BO_3$ | $SrCl_2$ | NaF |
|------|------|------|------|------|------|------|------|------|
| 24.53 | 5.2 | 4.09 | 1.16 | 0.695 | 0.201 | 0.027 | 0.025 | 0.003 |

## 3. RESULTS AND DISCUSSION

### 3.1. Microstructure and precipitation of experimental steels
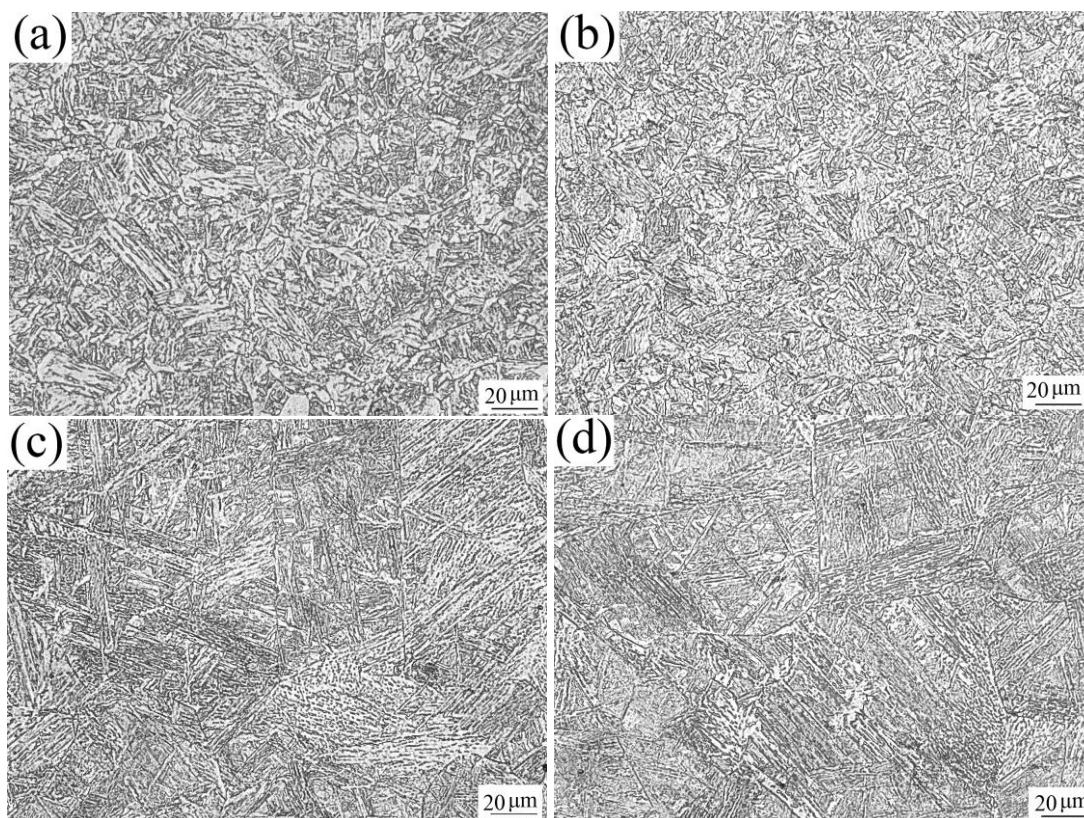


**Figure 1.** Microstructures of samples (a) N1: Nb-free steel; (b) N2: Nb-bearing steel 1# ; (c)N3: Nb-bearing steel 2# quenched at 1300°C; (d)N4: Nb-bearing steel 2# quenched at 1000°C

The microstructures of the produced steel (N1 and N2) and heat-treated steel (N3 and N4) are shown in Fig. 1. Fig. 1 (a) and Fig. 1 (b) are OM microstructures of Nb-free and Nb-bearing 1# steel respectively. Regardless of whether Nb is added, both sample N1 and N2 consist of granular bainite (GB). Moreover, the grain size of Nb-bearing steel is slightly finer than the Nb-free steel, which is consistent with previous reports that Nb refines grains and the uniform microstructure of alloy steel [8,9].

Sample N3 and N4 experienced high temperature austenitizing. Therefore, the grains were coarsened severely and composed of granular bainite and some lath bainite with coarse primary austenite grain boundaries, as shown in Fig. 1 (c) and Fig. 1 (d). Although quenched at different temperatures of austenitized zone, Samples N3 and N4 possess similar grain size and microstructures due to the same austenitizing temperature of 1300°C.

The nano-sized precipitates of samples were characterized by HRTEM as shown in Fig. 2. No obvious precipitation was observed in Nb-free samples, as shown in Fig.2 (a), while fine, well-distributed precipitates are observed in Nb-bearing samples, as shown in Fig.2 (b). The different quenching temperatures of samples N3 and N4 with the same Nb content resulted in a distinct difference in the precipitates of each sample. When Nb-bearing steel was heated to 1300°C, higher than the solution temperature of Nb carbide precipitates, and quenched directly to room temperature, the dissolved Nb carbide had no time to precipitate. Whereas, when the steel was heated to 1300°C, and held for 1 hour at 1000°C, the dissolved Nb carbide could precipitate effectively [10,13,14]. Once quenched to room temperature, a large number of precipitates were obtained in steel, as shown in Fig. 2 (d). The precipitates were indexed as Nb carbide precipitates, and the size of the major precipitates ranged from about 3 to 10 nm. On the other hand, observation of TEM revealed that the matrix of granular bainite in samples is bainite ferrite (BF) dispersed with nanosized carbide precipitates.
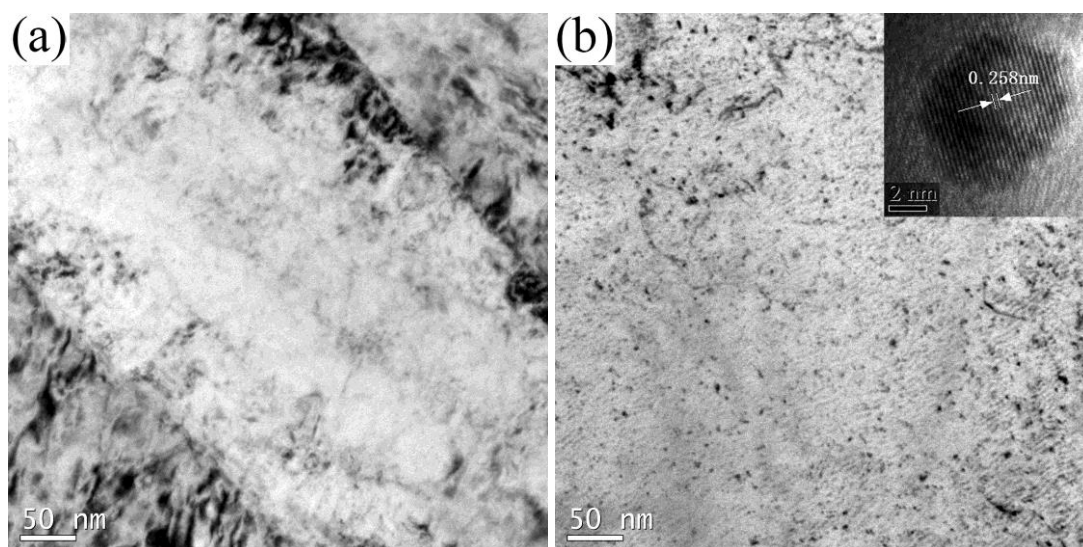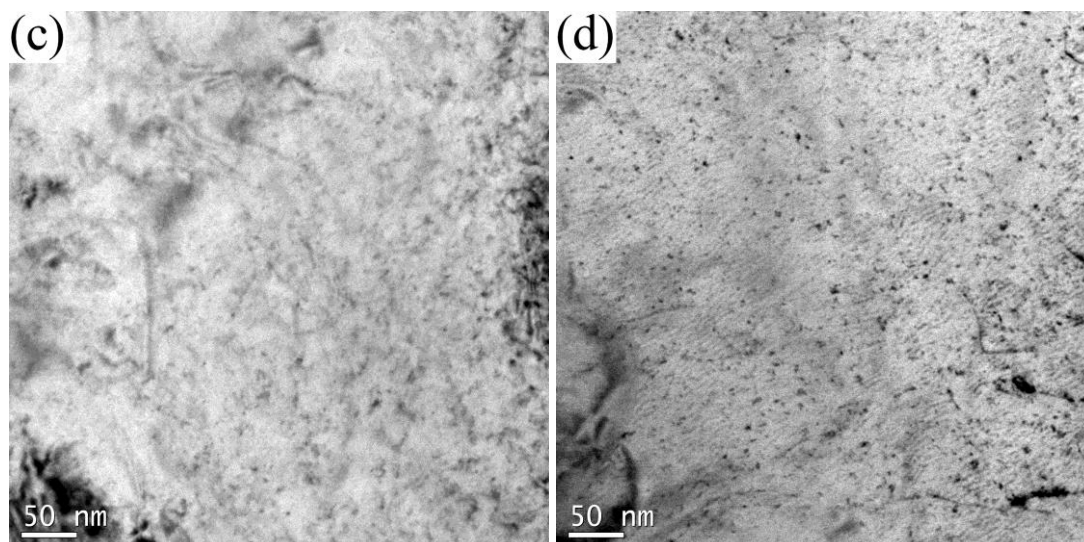
**Figure 2.** TEM micrographs of nano-sized precipitates in samples (a) N1: no precipitate; (b) N2: fine and well-distributed precipitates; (c) N3: few precipitates; (d) N4: fine, well-distributed precipitates.

### 3.2. Electrochemical analysis

The OCP of samples in simulated seawater are presented in Fig. 3. On the whole, the values of open circuit potential decrease with time. When the OCP reached a stable stage, the potential of Nb-bearing sample was more positive than for Nb-free sample, as shown in Fig. 3 (a). However, with the same content, similar grain size, microstructures, and different number of precipitates, the OCP of N3 and N4 were nearly equal, as shown in Fig. 3 (b). The results revealed that element Nb slightly affects OCP of the experimental steel, and Nb precipitates have little effect.
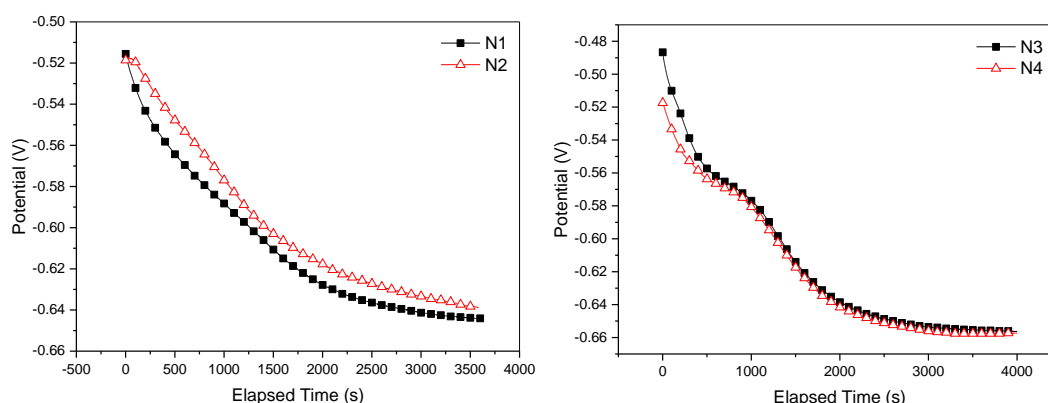


**Figure 3.** OCP of sample N1-N4 in simulated seawater

Fig. 4 shows the potential dynamic polarization curves in simulated seawater, revealing that all samples in simulated seawater manifested as the anodic process in an active state and the cathodic process dominated by an oxygen reduction reaction. Table 3 gives the electrochemical parameters

fitted from the potentiodynamic polarization curves in Fig.4. From Fig.4, the potential dynamic polarization curves of Nb-bearing steel (N1) and Nb-free steel (N2) are very similar. Based on electrochemical parameters from Table 3, the corrosion potential, $E_{corr}$ of Nb-bearing steel is slightly more positive than for Nb-free steel, and the corrosion current density, $i_{corr}$ of Nb-bearing steel is lower than for Nb-free steel. The results showed that the corrosion-resistance of HSLA steel in simulated seawater was improved by the addition of Nb[15], but the effect was limited, i.e., the microalloying element Nb induces a very limited effect on the corrosion behavior of HSLA steel in simulated seawater. From Table 3, the values of $E_{corr}$ and $i_{corr}$ of N3 and N4, which have the same Nb content, and different Nb carbide precipitates, were nearly the same. Therefore, based on the results of polarization curves, the nano-sized precipitates have no obvious effect on the corrosion behavior of HSLA steel in simulated seawater. Some researchers [16,17] reported that fine phases, including inclusion and precipitated particles, were innocuous or substantially beneficial to corrosion while the phase size remains well below 1 μm, in agreement with the results of sample N3 and N4. However comparing N1 and N2 to N3 and N4, the $i_{corr}$ of as-produced samples (N1 and N2) is much larger than for heat-treated samples (N3 and N4), revealing that the effect of microstructure on corrosion of the HSLA steel is much more remarkable than for microcontented Nb and nanosized precipitates.
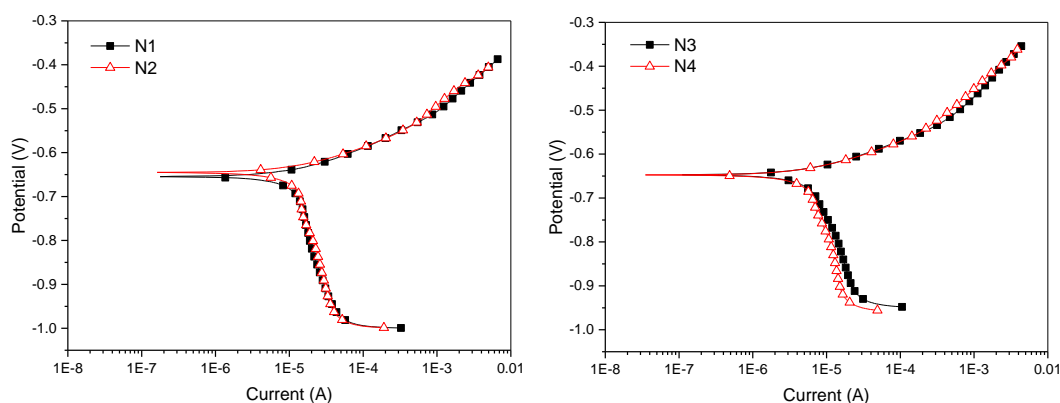


**Figure 4.** Potential dynamic polarization curves of sample N1-N4 in simulated seawater

**Table 3.** Electrochemical parameters fitted from potentiodynamic polarization curves in Fig.4

|  | N1 | N2 | N3 | N4 |
|---|---|---|---|---|
| $E_{corr}$/V$_{SCE}$ | -0.655 | -0.645 | -0.648 | -0.649 |
| $i_{corr}$/μAcm$^{-2}$ | 13.96 | 12.64 | 6.64 | 6.30 |

Fig. 5 shows Nyquist plots for the EIS tests performed on the samples at OCP in simulated seawater. The impedance arc radius of N2 is larger than for N1, and N3 and N4 have almost the same radius. The size of the impedance arc radius reflects corrosion resistance. ZSimpWin 3.50 was used to fit the EIS data, and the equivalent circuit is shown in Fig. 6. In the equivalent circuit, $R_s$ and $R_t$ represents solution resistance and charge-transfer resistance respectively, $R_f$ and $Q_f$ represents charge

transfer resistance and capacitance introduced by oxidation films, and $Q_{dl}$ represents the electrical double-layer capacitor of metal interfaces. In this environment, Rt reveals the corrosion resistance, that is, the corrosion resistance increases as Rt increases. Table 4 shows the relevant fitting parameters from the above equivalent circuit. It is obvious that the value of charge-transfer resistance of N2 (Nb-bearing steel) is much higher than for N1 (Nb-free steel), and the values of Rt of N3 and N4 are nearly equal, in accordance with potentiodynamic tests[18].
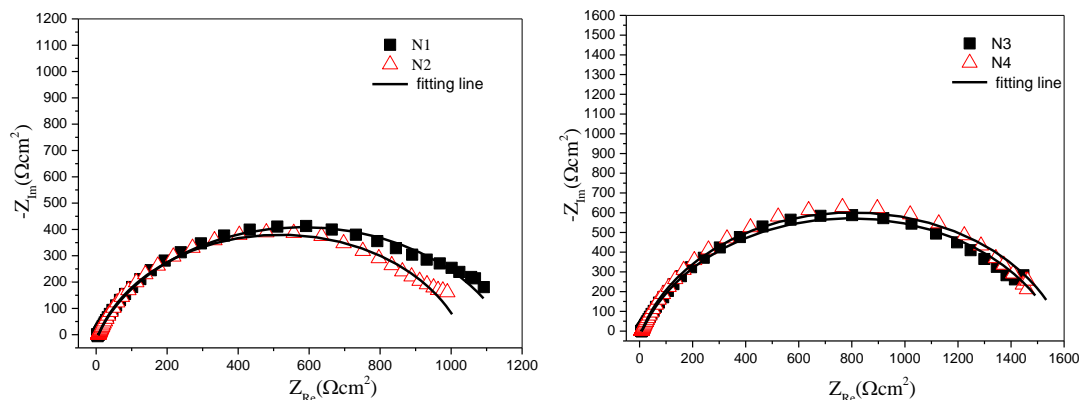


**Figure 5.** Nyquist plots of experimental steels
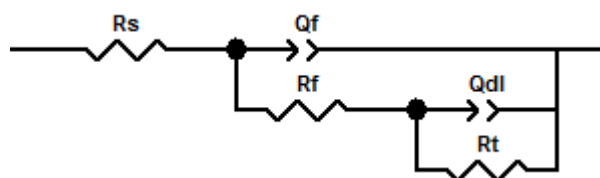


**Figure 6.** Equivalent circuit R(Q(R(QR))) of EIS

**Table 4.** Relevant parameters fitted from equivalent circuit

|  | N1 | N2 | N3 | N4 |
|---|---|---|---|---|
| $Rs(\Omega \cdot cm^2)$ | 5.904 | 5.887 | 7.415 | 6.559 |
| $Q_f(\mu F \cdot cm^2 \cdot s^{n-1})$ | $4.786 \times 10^{-5}$ | $2.701 \times 10^{-4}$ | $4.152 \times 10^{-4}$ | $3.968 \times 10^{-4}$ |
| $R_f(\Omega \cdot cm^2)$ | 1.178 | 5.087 | 19.50 | 18.88 |
| $Q_{dl}(\mu F \cdot cm^2 \cdot s^{n-1})$ | $8.457 \times 10^{-4}$ | $4.969 \times 10^{-4}$ | $3.789 \times 10^{-4}$ | $2.961 \times 10^{-4}$ |
| $Rt(\Omega \cdot cm^2)$ | 1155 | 1024 | 1547 | 1570 |

According to the results, Nb-bearing steel had higher corrosion resistance than Nb-free steel. The factors improving corrosion resistance include more homogeneous microstructure, lower carbon supersaturation and internal stress resulting from NbC, precipitation in Nb-bearing steel. Although NbC precipitates act as nano-scaled cathodic phases, no harmful or beneficial effects were presented

on the macro-scaled corrosion behavior of HSLA steel in simulated seawater. Whereas, the effect of microstructure on corrosion is more remarkable than for microcontented Nb and nanosized precipitates.

## 4. CONCLUSIONS

Nano-sized Nb carbide precipitates, which are usually applied as a strengthening and toughening phase in high-strength low-alloy steel, were revealed to play a substantially beneficial role on the corrosion resistance of HSLA steel in simulated seawater. Due to the more homogeneous microstructure, and lower carbon supersaturation and internal stress resulting from NbC precipitation, Nb-bearing HSLA steel possessed higher corrosion resistance. NbC precipitates acting as a nano-scaled cathodic phase, present no harmful, even beneficial effect on the macro-scaled corrosion behavior of HSLA steel.

## References

1. Z. Hu, G. Xu and H. Yang, *J. Mater. Eng. Perform.*, 12 (2014) 4216.
2. X. Chen, G. Qiao, X. Han, X. Wang, F. Xiao and B. Liao, *Mater. Design*, 53 (2014) 888.
3. B. Show, R. Veerababu, R. Balamuralikrishnan and G. Malakondaiah. *Mater. Sci. Eng. A*, 527 (2010) 1595.
4. S. Jeng, H. Lee, J. Huang and R. Kuo, *Mater. Trans.*, 49 (2008) 1270.
5. Z.,Xie X. Ma, C. Shang, X. Wang and S. Subramanian, *Mater. Sci. Eng. A*, 641 (2015) 37.
6. Y. Chen, D. Zhang, Y. Liu, H. Li and D. Xu, *Mater. Charact.*, 84 (2013) 232.
7. Q. Yu, Z. Wang, X. Liu and G. Wang, *Mater. Sci. Eng. A*, 379 (2004) 384.
8. S. Zhang, Y. Huang, B. Sun, Q. Liao, H. Lu, B. Jian, H. Mohrbacher, W. Zhang, A. Guo and Y. Zhang, *Mater. Sci. Eng. A*, 626 (2015) 136.
9. A. Farahat and T. El-Bita, *Mater. Sci. Eng. A*, 527 (2010) 3662.
10. S. Lu, S. Wei, D. Li and Y. Li, *J. Mater. Sci.*, 45 (2010) 2390.
11. P. Zhao, C. Cheng, G. Gao, W. Hui, R. Misra, B. Bai and Y. Weng, *Mater. Sci. Eng. A.*, 650 (2015) 438.
12. A. Kalashami, A. Kermanpur, E. Ghassemali, A. Najafizadeh and Y. Mazaheri, *Mater. Sci. Eng. A.* 678 (2016) 215.
13. A. Kostryzhev, P. Mannan and O. Marenych, *J. Mater. Sci.*, 50 (201) 7115.
14. S. Hong, H. Jun, K. Kang and C. Park, *Scripta Mater.*, 48 (2003) 1201.
15. J. Wei and B. Zhou. *Int.J. Electrochem. Sci.*, 12(2017) 3169.
16. T. Suter and H. Böhni, *Electrochim. Acta*, 42 (1997) 3275.
17. J. Stewart and D. Williams, ChemInform Abstract: *ChemInform.*, 15 (1992) 457.
18. L. Kong, K. Wang, Y. Zhan, and Y. Zhang, *Int. J. Electrochem. Sci.*, 12(2017) 2982.